Conformational Stability From Temperature-Dependent Fourier Transform Infrared Spectra Of Noble Gas Solutions, r_0 Structural Parameters, and Barriers To Internal Rotation for Ethylamine†

James R. Durig,* Chao Zheng, and Todor K. Gounev

Department of Chemistry, University of Missouri-Kansas City, Kansas City, Missouri 64110

Wouter A. Herrebout and Benjamin J. van der Veken

Department of Chemistry, University of Antwerp, Groenenborgerlaau 171, B2020 Antwerp, Belgium

Received: December 14, 2005; In Final Form: February 22, 2006

Variable temperature (−55 to −145 °C) studies of the infrared spectra (3500 to 100 cm^{-1}) of ethylamine, $CH_3CH_2NH_2$, dissolved in liquid krypton and/or xenon have been recorded. From these data, the enthalpy differences have been determined to be 54 ± 4 cm^{-1} (0.65 ± 0.05 kJ/mol), with the trans conformer (methyl group relative to the lone pair of electrons on nitrogen) being the more stable form. It is estimated that there is 61 ± 1% of the doubly degenerate gauche form present at ambient temperature. The conformational energetics have been calculated with the Møller−Plesset perturbation method to the second order (MP2(full)) and the fourth order (MP4(SDTQ)) as well as with density functional theory by the B3LYP method utilizing a variety of basis sets. Basis sets with diffuse functions lead to incorrect prediction of the conformational stability. On the basis of the frequencies of the torsional transitions along with the determined experimental enthalpy difference and gauche dihedral angle, the potential function governing conformational interchange has been obtained, and the determined Fourier cosine coefficients are $V_1 = -207 \pm 48$, $V_2 = 320 \pm 67$, $V_3 = 1072 \pm 25$, $V_4 = 55 \pm 11$, and $V_5 = -96 \pm 28$ cm^{-1}, with a trans-to-gauche barrier of 1286 cm^{-1}, and a gauche-to-gauche barrier of 715 cm^{-1}. The 3-fold methyl rotational barriers have been determined to be 1241 ± 4 and 1281 ± 10 cm^{-1} for the gauche and trans conformers, respectively. By utilizing the previously reported microwave rotational constants combined with the structural parameters predicted at the MP2(full)/6-311+G(d,p) level, adjusted r_0 structural parameters have been obtained. A complete vibrational assignment is given for the trans conformer, which is supported by normal coordinate calculations utilizing scaled force constants from ab initio B3LYP/6-311++G(3df,3pd) calculations. Proposed assignments are also made for the fundamentals of the gauche conformer. The results of these spectroscopic and theoretical studies are discussed and compared to the corresponding results for similar molecules.

Introduction

There have been several determinations of the enthalpy difference between the proposed more stable trans conformer of ethylamine, $CH_3CH_2NH_2$, and the high-energy gauche rotamer. An estimate of the enthalpy difference of 207 cm^{-1} (2.27 kJ/mol) was made[1] from the potential function obtained by fitting the asymmetric torsional transitions observed in the Raman spectrum of the gas. At about the same time, Tsuboi et al.[2] reported an estimate of the enthalpy difference of 230 cm^{-1} (2.75 kJ/mol) for the two conformers by fitting the far-infrared spectral data of ethylamine with a coupled two-rotor model for CH_3 and NH_2 tops. These results were significantly different from an earlier far-infrared study[3] in which the gauche conformer was predicted to be more stable with an enthalpy difference of 104 cm^{-1}. This value was in agreement with the earliest ab initio prediction[4] of the gauche form being more stable by 182 cm^{-1}. The conformational stability had not been experimentally determined at that time but it was reported[5] that both conformers were present in significant amounts. A decade later, an enthalpy difference between the two conformers of ethylamine was obtained from relative intensity measurements of the microwave spectra,[6] which gave a value of 110 ± 50 cm^{-1} (1.32 ± 0.60 kJ/mol), with the trans conformer being the more stable form. This result compared favorably with the value of 100 ± 10 cm^{-1} (1.20 ± 0.12 kJ/mol) obtained[7] from the infrared spectra of the variable temperature vapor deposited in an argon matrix. Although the latter value had a much lower uncertainty, the matrix technique can give enthalpy values significantly different from the vapor phase because of the effective temperature at the site of the deposition and the molecular orientation in the matrix. The most recent determination of the enthalpy difference was from a gas-phase electron diffraction study[8] in which a value of 107 ± 70 cm^{-1} (1.28 ± 0.84 kJ/mol) was obtained with the trans form being more stable, but with a very large uncertainty. Although the latter three experimental enthalpy differences are quite consistent with the values of about 100 to 110 cm^{-1}, two of the three determinations have very large uncertainties. These three conformational enthalpy differences are much smaller than those obtained from

* Corresponding author, phone: 01 816-235-6038, fax: 01 816-235-2290, email: durigj@umkc.edu.

† Taken in part from the thesis of C. Zheng, which will be submitted to the Department of Chemistry of the University of Missouri-Kansas City, Kansas City, MO, in partial fulfillment of the Ph.D. degree.

10.1021/jp057305q CCC: $33.50
Published on Web 04/07/2006

the fit of the torsional transitions,[1,2] and they are close to the value of 97 cm^{-1} (1.16 kJ/mol) predicted[9] from MP2/6-311G(d,p) ab initio calculations with frozen core electron correlation.

To obtain a more reliable experimental value for the conformational enthalpy difference of ethylamine, we have investigated the variable temperature (−55 to −145 °C) infrared spectra (3500 to 100 cm^{-1}) of a sample dissolved in liquid krypton and xenon. From ab initio B3LYP/6-311++G(3df,3pd) calculations, we have obtained the harmonic force fields, vibrational frequencies, infrared intensities, Raman activities, and depolarization ratios. We employed larger basis sets (up to 6-311+G-(2df,2pd)) as well as higher levels of electron correlation (MP4(SDTQ)) than those previously reported[9] to predict the conformational stabilities and structural parameters. Zero-point energy and thermal enthalpy corrections were calculated in addition to electronic energy. The predicted structural parameters at the MP2(full)/6-311+G(d,p) level have been systematically fitted to the previously reported[6,10,11] rotational constants of several isotopic substituted species to provide adjusted r_0 parameters for both conformers. The results of the spectroscopic and theoretical studies are reported herein.

Experimental Section

The sample of ethylamine was purchased from Aldrich Chemical Co., Milwaukee, WI, with a stated purity of 98%. The sample was further purified by means of a low-temperature, low-pressure fractionation column, and the purity was checked by a comparison of the infrared spectrum to those previously reported.[9,12−15]

The mid-infrared spectrum of gas was obtained from 3500 to 230 cm^{-1} on a Perkin-Elmer model 2000 Fourier transform spectrometer equipped with a Ge/CsI beam splitter and a DTGS detector. The theoretical resolution used to obtain the spectrum of the gas was 0.5 cm^{-1}. Sixty-four interferograms were added and transformed with a boxcar truncation function. The mid-infrared spectra (3500 to 400 cm^{-1}) (Figure 1A) of the sample dissolved in liquefied krypton (−105 to −145 °C) and xenon (−55 to −100 °C) as a function of temperature were recorded on a Bruker model IFS-66 Fourier transform spectrometer, as described[16] previously. In all cases, 100 interferograms were collected at a 1.0 cm^{-1} resolution, averaged, and transformed with a boxcar truncation function.

The far-infrared spectra (400 to 30 cm^{-1}) of the krypton solutions (−117.4 to −149.4 °C) (Figure 2D) were recorded on a Bruker model IFS-66 N/S Fourier transform spectrometer that was equipped with a Globar source, a 6.0 μm Mylar beam splitter, and a liquid helium-cooled silicon bolometer. The interferograms for these studies were recorded at a resolution of 0.5 cm^{-1} and were averaged over 250 scans and transformed by a Blackman−Harris apodization function.

The Raman spectra were recorded with a Spex model 1403 spectrophotometer equipped with a Spectra-Physics model 164 argon ion laser operating on the 5145 Å line. The laser power used was 0.5 W with an instrument resolution of 3 cm^{-1}. The spectra of the liquid and solid were recorded with the sample contained in sealed capillaries, with a Miller−Harney cell[17] used for the solid; a typical Raman spectrum of the liquid is shown in Figure 3A. The wavenumbers for the fundamentals for both the trans and gauche forms in the gas, noble gas solution, and solid are listed in Tables 1 and 2, respectively.

Ab Initio Calculations

The LCAO-MO-SCF restricted Hartree−Fock calculations were performed with the Gaussian 03 program[18] using Gaussian-type basis functions. The energy minima with respect to nuclear coordinates were obtained by the simultaneous relaxation of all geometric parameters using the gradient method of Pulay.[19] The 6-31G(d), 6-311G(d,p), 6-311G(2d,2p), and 6-311G(2df,2pd) basis sets as well as the corresponding ones with diffuse functions were employed with the Møller−Plesset perturbation method to the second order (MP2(full)) and the fourth order (MP4(SDTQ)), as well as with the density functional theory by the B3LYP method. The predicted conformational energy differences are listed in Table 3, as well as with zero-point energy and thermal enthalpy (at 298.15 K and 1 atm) corrections.

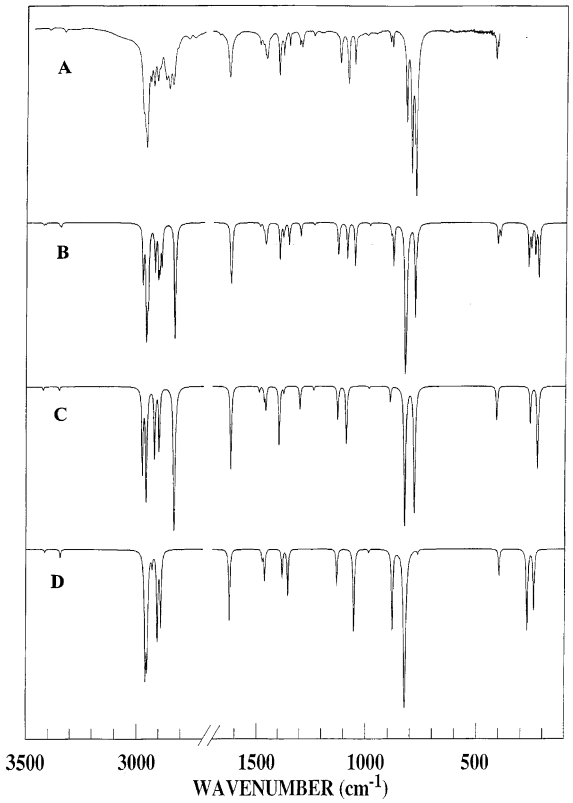

Figure 1. Comparison of experimental and calculated infrared spectra of ethylamine: (A) observed infrared spectrum of ethylamine in liquid krypton at −130 °C; (B) simulated infrared spectrum of a mixture of trans and gauche conformers at −130 °C with $\Delta H = 54$ cm^{-1}; (C) simulated infrared spectrum of a pure gauche conformer; (D) simulated infrared spectrum of a pure trans conformer.

To obtain a complete description of the molecular motions involved in the fundamental modes of ethylamine, a normal coordinate analysis has been carried out. The force field in Cartesian coordinates was obtained with the Gaussian 03 program at the B3LYP/6-311++G(3df,3pd) level. The internal coordinates used to calculate the **G** and **B** matrices are shown in Figure 4. By using the **B** matrix,[20] the force field in Cartesian coordinates was converted to a force field in internal coordinates. The force constants in internal coordinates for both the trans and gauche conformers are listed in Table 1S (Supporting Information). Subsequently, scaling factors of 0.92 for CH and NH stretches, 1.0 for CC and CN stretches and CCN bend, and 0.96 for all other coordinates were applied, along with the geometric average of scaling factors for interaction force constants, to obtain the fixed scaled force field and resultant wavenumbers. A set of symmetry coordinates was used (Table 2S, Supporting Information) to determine the corresponding potential energy distributions (PEDs). A comparison between the observed and calculated wavenumbers, along with the

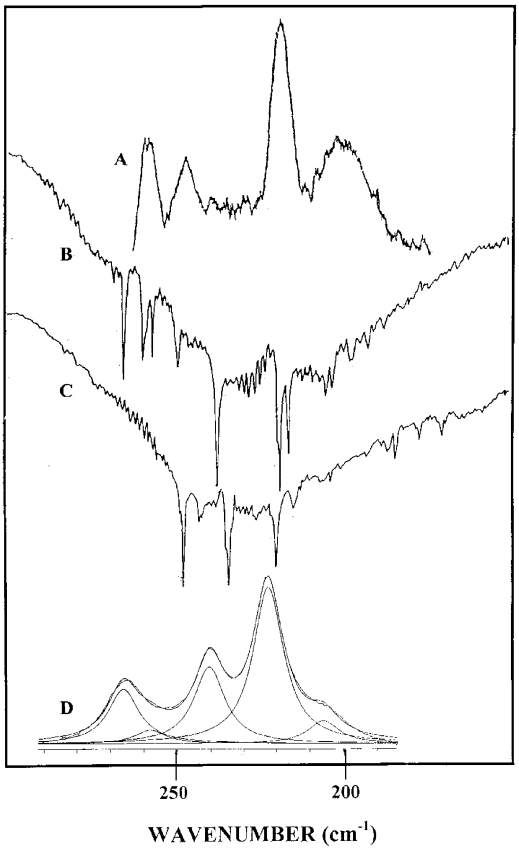

Figure 2. Low-frequency spectra of ethylamine: (A) Raman spectrum of the gas (ref 1); (B) infrared spectrum of the gas (ref 2); (C) infrared spectrum of $CD_3CH_2NH_2$ gas (ref 2); (D) infrared spectrum of krypton solution at −113 °C.

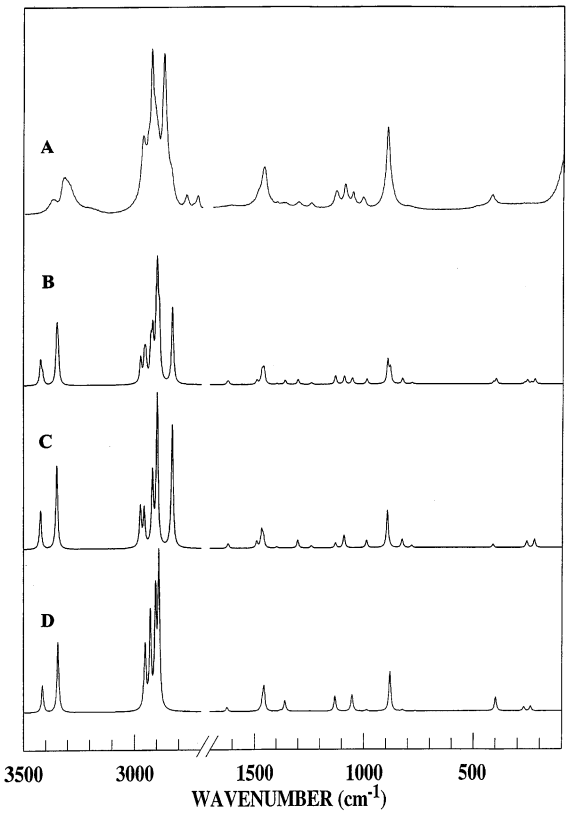

Figure 3. Comparison of experimental and calculated Raman spectra of ethylamine: (A) observed Raman spectrum of ethylamine in liquid phase at 20 °C; (B) simulated Raman spectrum of a mixture of trans and gauche conformers at 20 °C with $\Delta H = 54$ cm^{-1}; (C) simulated Raman spectrum of a pure gauche conformer; (D) simulated Raman spectrum of a pure trans conformer.

calculated infrared intensities, Raman activities, depolarization ratios, and PEDs for the trans and gauche conformers are listed in Tables 1 and 2, respectively.

The infrared spectra were predicted from the B3LYP/6-311++G(3df,3pd) calculations. The predicted scaled frequencies were used together with a Lorentzian function to obtain the calculated spectra. Infrared intensities determined from B3LYP/6-311++G(3df,3pd) calculations were obtained on the basis of the dipole moment derivatives with respect to Cartesian coordinates. The derivatives were transformed with respect to normal coordinates by $(\partial\mu_u/\partial Q_i) = \sum_j (\partial\mu_u/\partial X_j)\mathbf{L}_{ij}$, where Q_i is the ith normal coordinate, X_j is the jth Cartesian displacement coordinate, and $\mathbf{L}_{ij}$ is the transformation matrix between the Cartesian displacement coordinates and the normal coordinates. The infrared intensities were then calculated by $(N\pi)/(3c^2)$ $[(\partial\mu_x/\partial Q_i)^2 + (\partial\mu_y/\partial Q_i)^2 + (\partial\mu_z/\partial Q_i)^2]$. In panels D and C of Figure 1, the simulated infrared spectra of the pure trans and gauche conformers, respectively, are shown. The simulated spectra, calculated for −130 °C, of a mixture of two conformers with a ΔH of 54 cm^{-1} (experimental value, see Conformational Stability section), with the trans conformer being more stable, is shown in Figure 1B, and it should be compared to the experimental spectrum of the krypton solution at −130 °C (Figure 1A). The predicted spectrum is in good agreement with the experimental spectrum, which indicates the utility of the scaled predicted data in distinguishing the fundamentals for the two conformers.

To further support the vibrational assignments, we have simulated the Raman spectra from the ab initio B3LYP/6-311++G(3df,3pd) results. The evaluation of Raman activity by using the analytical gradient methods has been developed.[21,22] The activity S_j can be expressed as $S_j = g_j(45\alpha_j^2 + 7\beta_j^2)$, where g_j is the degeneracy of the vibrational mode j, α_j is the derivative of the isotropic polarizability, and β_j is that of the anisotropic polarizability. To obtain the polarized Raman scattering cross sections, the polarizabilities are incorporated into S_j by multiplying S_j with $(1 - \rho_j)/(1 + \rho_j)$, where ρ_j is the depolarization ratio of the jth normal mode. The Raman scattering cross sections and calculated wavenumbers obtained from the Gaussian 03 program were used together with a Lorentzian function to obtain the simulated Raman spectra.

The simulated Raman spectra of the pure trans and gauche conformers are shown in Figure 3, panels D and C, respectively. The simulated Raman spectra, calculated for 25 °C, of a mixture of two conformers with a ΔH of 54 cm^{-1}, is shown in Figure 3B. The experimental Raman spectrum of the liquid is shown in Figure 3A for comparison, and the agreement is considered satisfactory, but not nearly as good as that of the infrared spectrum, probably due, in part, to intermolecular association in the liquid phase.

Vibrational Assignment

To determine the conformational stabilities of ethylamine, it is necessary to confidently assign bands to the trans and gauche conformers. By using ab initio predicted frequencies, infrared gas-phase band contours, and band intensities from the infrared and Raman spectra, it was possible to provide reasonably complete vibrational assignments for both conformers. Because the rotation of the NH_2 group has little effect on the moments of inertia of ethylamine, the predicted gas-phase infrared band contours for the trans and gauche forms are almost the same

TABLE 1: Observed and Calculated Frequencies for trans Ethylamine

		fundamental	ab initio[a]	fixed scaled[b]	IR int.[c]	Raman act.[d]	dp ratio	IR gas	IR rare gas solution	Raman liquid	Raman solid	PED[e]	A[f]	B[f]	C[f]
A′	ν_1	NH_2 symmetric stretch	3486	3344	2.0	117.7	0.07	3344	3331	3320	3175	$100S_1$	41	59	
	ν_2	CH_3 antisymmetric stretch	3078	2952	47.3	83.2	0.58	2967	2962	2963	2959	$98S_2$	33	67	
	ν_3	CH_2 symmetric stretch	3028	2905	30.5	146.2	0.11		2913	2914	2916	$98S_3$	0	100	
	ν_4	CH_3 symmetric stretch	3013	2890	23.8	194.5	0.01	2878	2874	2870	2867	$100S_4$	77	23	
	ν_5	NH_2 deformation	1658	1624	21.9	2.3	0.72	1626	1620	1611	1628	$74S_5$, $25S_{13}$	5	95	
	ν_6	CH_2 deformation	1505	1475	2.5	0.5	0.59	1465	1467	1468	1465	$60S_6$, $34S_7$	5	95	
	ν_7	CH_3 antisymmetric deformation	1487	1457	0.3	10.7	0.72	1456	1453	1453	1441	$57S_7$, $39S_6$	51	49	
	ν_8	CH_3 symmetric deformation	1408	1381	7.3	0.3	0.27	1378	1374	1374	1371	$95S_8$	78	22	
	ν_9	CH_2 wag	1383	1355	12.7	0.3	0.02	1350	1347	1354	1349	$91S_9$	99	1	
	ν_{10}	CH_3 rock	1142	1130	9.7	5.1	0.20	1117	1116	1124	1148	$35S_{10}$, $22S_{12}$, $15S_{14}$, $11S_{11}$	2	98	
	ν_{11}	CCN antisymmetric stretch	1056	1053	26.8	5.1	0.49	1055	1052	1048	1051	$87S_{11}$, $10S_{10}$	100	0	
	ν_{12}	CCN symmetric stretch	890	880	26.0	9.6	0.20	882	881	891	872	$40S_{12}$, $36S_{10}$, $15S_{13}$	92	8	
	ν_{13}	NH_2 wag	835	823	141.5	0.3	0.75	789	795	~802		$49S_{13}$, $33S_{12}$, $17S_5$	98	2	
	ν_{14}	CCN bend	401	399	6.8	1.2	0.20	404	406	415	423	$82S_{14}$	91	9	
A″	ν_{15}	NH_2 antisymmetric stretch	3560	3414	0.8	46.5	0.75	3413	3400	3366	3324	$100S_{15}$			100
	ν_{16}	CH_3 antisymmetric stretch	3086	2960	57.8	4.8	0.75	2968	2961	2963	2959	$73S_{16}$, $27S_{17}$			100
	ν_{17}	CH_2 antisymmetric stretch	3054	2929	3.1	124.5	0.75	2921	2929	2929	2926	$73S_{17}$, $27S_{16}$			100
	ν_{18}	CH_3 antisymmetric deformation	1494	1464	7.9	4.1	0.75	1459	1458	1452	1448	$91S_{18}$			100
	ν_{19}	CH_2 twist	1387	1360	0.1	4.3	0.75	1350	1347	1354	1349	$58S_{19}$, $34S_{21}$			100
	ν_{20}	CH_3 rock	1269	1244	0.1	0.2	0.75	1238	1235	1238	1249	$27S_{20}$, $23S_{21}$, $22S_{22}$, $22S_{19}$			100
	ν_{21}	NH_2 twist	1006	986	0.9	0.4	0.75	993	995	1003		$38S_{21}$, $31S_{20}$, $16S_{19}$, $12S_{22}$			100
	ν_{22}	CH_2 rock	781	765	1.0	0.1	0.75					$56S_{22}$, $32S_{20}$			100
	ν_{23}	CH_3 torsion	278	272	26.1	0.2	0.75	265	266	~270	278	$40S_{23}$, $56S_{24}$			100
	ν_{24}	NH_2 torsion	247	242	17.4	0.2	0.75	237	240		383	$41S_{24}$, $57S_{23}$			100

[a] Calculated at the B3LYP/6-311++G(3df,3pd) level. [b] With scaling factors of 0.92 for CH and NH stretches, 1.0 for CC and CN stretches and the CCN bend, and 0.96 for all other modes. [c] Calculated infrared intensities in km/mol. [d] Calculated Raman activities in $Å^4$/u. [e] Values less than 10% are omitted. [f] Percentage of A-, B-, and C-type gas-phase infrared band contours.

(Figure 1S, Supporting Information). However, for both conformers, the B- and C-type contours exhibit significantly larger rotational spacing than do the A-type band envelopes. For the trans conformer, the *a* and *b* principle axes lie in the molecular plane of symmetry, and, thus, all fundamentals of the A′ species are expected to give rise to A/B hybrid contours, whereas all fundamentals of the A″ species are expected to give rise to a pure C-type contour. In addition, all fundamentals of the A′ species of the trans conformer are expected to be polarized, and those of the A″ species are expected to be depolarized in the Raman effect.

In one of the most recent vibrational assignments[23] for ethylamine, which included ab initio MP2(frozen core)/6-311G-(d,p) predictions utilizing previously reported spectral data,[12−15] seven of the fundamentals of the trans conformer in the fingerprint region were not assigned and were listed as "no experimental data available", which agrees with the assignment provided by Hamada et al.[7] The inability to identify the fundamentals for the trans conformer arises from the large amount of the gauche form present at ambient temperatures, with many of the fundamentals at nearly the same frequency as the corresponding modes of the trans form. However, by utilizing the spectral data from the low-temperature noble gas solutions, many of these near-degenerate bands can be resolved (Figures 1, 2, and 5). For example, in the far-infrared spectrum of the gas, where the NH_2 and CH_3 torsions have been assigned[7] at 259 and 218 cm^{-1} for the gauche conformer, there are four well-defined bands in the spectra of krypton solutions at 266, 258, 240, and 223 cm^{-1} (Figure 2) as well as a shoulder at 212 cm^{-1}, which are expected to arise from these two fundamentals for both conformers. This is a clear illustration of the advantage of using low-temperature spectral data from rare gas solutions for assigning strongly overlapping bands, and similar results are also obtained from the spectra in the fingerprint region (Figure 5). Therefore, it has been possible to assign all seven of these previously unassigned fundamentals in the "fingerprint" region for the trans conformer.

The seven unassigned fundamentals in this spectral region were the NH_2 deformation (scissors), CH_2 deformation (scissors), CH_2 wag, CH_2 twists, CH_3 rock, NH_2 twist, and CCN bend. For the trans form, these modes can be assigned at 1626, 1465, 1350 (2), 1117, 993, and 404 cm^{-1}, respectively, from the spectrum of the gas, particularly when it is realized that some of the corresponding modes for the gauche rotamer are either predicted with distinctively different gas-phase infrared band envelopes or have very little predicted intensity, so that

TABLE 2: Observed and Calculated Frequencies for gauche Ethylamine

	fundamental	ab initio[a]	fixed scaled[b]	IR int.[c]	Raman act.[d]	dp ratio	IR gas	IR rare gas solution	Raman liquid	PED[e]	A[f]	B[f]	C[f]
ν_1	NH_2 symmetric stretch	3492	3350	1.0	139.4	0.08	3344	3331	3320	$99S_1$	7	7	86
ν_2	CH_3 antisymmetric stretch	3102	2975	28.8	53.5	0.75	2985	2977		$56S_2$, $43S_{16}$	11	35	54
ν_3	CH_2 symmetric stretch	2950	2830	83.1	153.1	0.23		2842	2842	$61S_3$, $38S_{17}$	4	63	33
ν_4	CH_3 symmetric stretch	3023	2899	18.9	196.6	0.02	2878	2874	2870	$93S_4$	70	25	5
ν_5	NH_2 deformation	1652	1619	27.3	2.5	0.71	1622	1620	1611	$74S_5$, $25S_{13}$	53	4	43
ν_6	CH_2 deformation	1521	1490	1.4	3.1	0.75	1486	1482	1477	$85S_6$, $11S_7$	39	51	10
ν_7	CH_3 antisymmetric deformation	1498	1468	3.2	8.0	0.75	1465	1467	1468	$77S_7$, $13S_6$	54	39	7
ν_8	CH_3 symmetric deformation	1404	1376	1.5	0.1	0.62	1378	1374	1374	$73S_8$, $22S_9$	4	93	3
ν_9	CH_2 wag	1424	1397	17.0	0.6	0.28	1397	1395	1392	$54S_9$, $24S_8$, $12S_{21}$	100	0	0
ν_{10}	CH_3 rock	1148	1128	8.8	1.6	0.25	1117	1116	1124	$17S_{10}$, $29S_{22}$, $18S_{20}$	0	36	64
ν_{11}	CCN antisymmetric stretch	1093	1089	16.6	4.1	0.64	1085	1082	1084	$77S_{11}$	88	11	1
ν_{12}	CCN symmetric stretch	897	891	3.7	9.3	0.14	892	891	891	$72S_{12}$, $17S_{10}$	2	47	51
ν_{13}	NH_2 wag	840	824	75.0	1.9	0.44	773	777		$37S_{13}$, $22S_{20}$, $13S_5$	20	44	36
ν_{14}	CCN bend	413	411	8.9	0.3	0.59	413	413	415	$81S_{14}$	73	0	27
ν_{15}	NH_2 antisymmetric stretch	3569	3423	1.0	66.3	0.68	3413	3400	3366	$99S_{15}$	18	50	32
ν_{16}	CH_3 antisymmetric stretch	3084	2958	46.5	49.6	0.39	2967	2961	2963	$48S_{16}$, $42S_2$	16	34	50
ν_{17}	CH_2 antisymmetric stretch	3044	2920	21.9	93.6	0.59	2921	2929	2926	$55S_{17}$, $35S_3$	8	52	40
ν_{18}	CH_3 antisymmetric deformation	1490	1460	5.7	5.2	0.72	1456	1453	1452	$89S_{18}$	1	2	97
ν_{19}	CH_2 twist	1327	1301	5.9	3.2	0.70	1293	1291	1297	$66S_{19}$, $14S_{21}$	79	15	6
ν_{20}	CH_3 rock	1262	1238	1.1	0.9	0.23	1238	1235	1238	$19S_{20}$, $27S_{21}$, $15S_{22}$, $12S_{19}$	52	34	14
ν_{21}	NH_2 twist	1002	986	0.7	2.1	0.36	993	995	1003	$32S_{21}$, $30S_{10}$, $13S_{11}$	30	70	0
ν_{22}	CH_2 rock	797	781	57.7	0.5	0.37	816	817		$39S_{22}$, $23S_{13}$, $21S_{20}$	12	42	46
ν_{23}	CH_3 torsion	266	260	9.7	0.3	0.42	259	258	~270	$64S_{23}$, $29S_{24}$	54	25	21
ν_{24}	NH_2 torsion	230	226	26.9	0.3	0.42	218	223		$65S_{24}$, $33S_{23}$	30	46	24

[a] Calculated at the B3LYP/6-311++G(3df,3pd) level. [b] With scaling factors of 0.92 for CH and NH stretches, 1.0 for CC and CN stretches and the CCN bend, and 0.96 for all other modes. [c] Calculated infrared intensities in km/mol. [d] Calculated Raman activities in $Å^4$/u. [e] Values less than 10% are omitted. [f] Percentage of A-, B-, and C-type gas-phase infrared band contours.

the band observed is for the trans conformer rather than the gauche form. The *Q*-branch at 1622 cm^{-1} must be due to the gauche conformer with a predicted 53% A/43% C-type contour, whereas this fundamental for the trans conformer is predicted to have a B-type contour (95%) and at a 3 cm^{-1} higher frequency. The ab initio predicted frequency can also be used for the CCN bend (ν_{14}), which is predicted to appear at 399 cm^{-1} (91% A-type and 9% B-type; observed at 404 cm^{-1}) for the trans conformer and 411 cm^{-1} (73% A-type and 27% C-type; observed at 413 cm^{-1}) for the gauche form. However, only one band at 415 cm^{-1} is observed in the Raman spectrum of the liquid for these two fundamentals. The 1350 cm^{-1} band was previously assigned[7,23] as the CH_3 symmetric deformation of the trans conformer; however, it is better assigned as the CH_2 wag/CH_2 twist with the CH_3 symmetric deformation at 1378 cm^{-1}, in coincidence with the corresponding mode of the gauche rotamer. The most uncertain assignment of these seven modes is the NH_2 twist at 993 cm^{-1}, which is coincident with the corresponding mode for the gauche conformer, but it is the only band between the fundamentals at 1055 and 892 cm^{-1}. These twisting modes have previously been assigned[7] in the 1200 cm^{-1} region where a weak band at 1235 cm^{-1} has not been assigned. With the exception of this mode, the remaining fundamentals for the trans conformer are confidently assigned (Table 1). This leaves four bands at 1347, 1052, 881, and 795 cm^{-1} (from krypton solutions) of the trans conformer for conformational determinations, which are sufficiently displaced from the gauche fundamentals. The similar data for the gauche conformer are at 1395, 1291, 1082, 891, and 817 cm^{-1} (frequencies from krypton solution, Table 2) and are sufficiently displaced from the trans fundamentals for enthalpy difference determinations.

The heavy atom skeletal stretching and bending modes are among the most sensitive to conformation. The CCN antisymmetric stretch (ν_{11}) is predicted at 1053 cm^{-1} for the trans conformer and at 1089 cm^{-1} for the gauche form from the fixed-scaled ab initio force field. The higher frequency band with a near A-type gas-phase contour (*Q*-branch at 1085 cm^{-1}) is confidently assigned as ν_{11} of the gauche conformer, whereas the lower frequency *Q*-branch at 1055 cm^{-1} is assigned as the CCN antisymmetric stretch of the trans conformer. The gauche band at 1084 cm^{-1} disappears in the Raman spectrum of the crystalline solid, leaving only the trans band at 1051 cm^{-1}, which clearly indicates that the trans conformer is the only form remaining in the crystalline solid. Finally, it is worth noting that, because of strong hydrogen bonding in the crystal, the NH_2 torsional mode experiences a large frequency shift in going from a gas (237 cm^{-1}) to a solid (383 cm^{-1}).

Conformational Stabilities

To obtain an accurate determination of the enthalpy difference between the two conformers, the mid-infrared spectra of

TABLE 3: Calculated Energy Differences[a] (cm^{-1}) between the trans and gauche Conformations of Ethylamine

method/basis	ΔE (electronic)	ΔE (electronic + zero-point energy)	ΔH (electronic + thermal enthalpy) at 298.15 K
MP2(full)/6-31G(d)	72	72	78
MP2(full)/6-31+G(d)	−65	−53	−52
MP2(full)/6-311G(d,p)	96	95	102
MP2(full)/6-311+G(d,p)	−64	−37	−40
MP2(full)/6-311G(2d,2p)	32	46	49
MP2(full)/6-311+G(2d,2p)	−66	−47	−47
MP2(full)/6-311G(2df,2pd)	29	48	52
MP2(full)/6-311+G(2df,2pd)	−59	−41	−41
B3LYP/6-31G(d)	151	143	147
B3LYP/6-31+G(d)	25	24	27
B3LYP/6-311G(d,p)	126	121	126
B3LYP/6-311+G(d,p)	3	11	11
B3LYP/6-311G(2d,2p)	104	105	109
B3LYP/6-311+G(2d,2p)	5	8	10
B3LYP/6-311G(2df,2pd)	94	97	102
B3LYP/6-311+G(2df,2pd)	3	4	7
MP4(SDTQ)/6-31G(d)	99		
MP4(SDTQ)/6-31+G(d)	−36		
MP4(SDTQ)/6-311G(d,p)	128		
MP4(SDTQ)/6-311+G(d,p)	−38		
MP4(SDTQ)/6-311G(2d,2p)	62		
MP4(SDTQ)/6-311+G(2d,2p)	−39		

[a] Energies of the gauche form relative to the trans form; a negative value indicates that the gauche form is predicted to be more stable. Experimental $\Delta H = 54 \pm 4$ cm^{-1}.

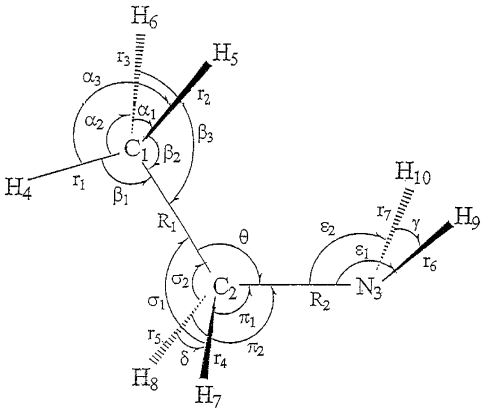

Figure 4. Geometric model and internal coordinates of ethylamine.

ethylamine dissolved in liquefied krypton as a function of temperature from −105 to −145 °C have been recorded, along with similar temperature-dependent studies in liquid xenon from −55 to −100 °C. In addition, the far-infrared spectra of ethylamine dissolved in liquefied krypton as a function of temperature from −117.4 to −149.4 °C have been recorded. Small interactions are expected to occur between the dissolved sample and the surrounding noble gas atoms, and, consequently, small frequency shifts are anticipated when passing from the gas phase to the liquefied noble gas solutions.[24−27] A significant advantage of such temperature studies in noble gas solutions is that the conformer bands are better resolved in comparison with those in the spectrum of the gas (Figure 5). Also, the intensities of the conformer peaks are more accurately determined compared to those from the spectrum of the gas because of the absence of rotational fine structure. In the noble gas solutions of ethylamine, the major intermolecular force is the dipole-induced dipole interaction between this molecule and surrounding noble gas atoms. From ab initio calculations, the dipole moments of the two conformers are predicted to have similar

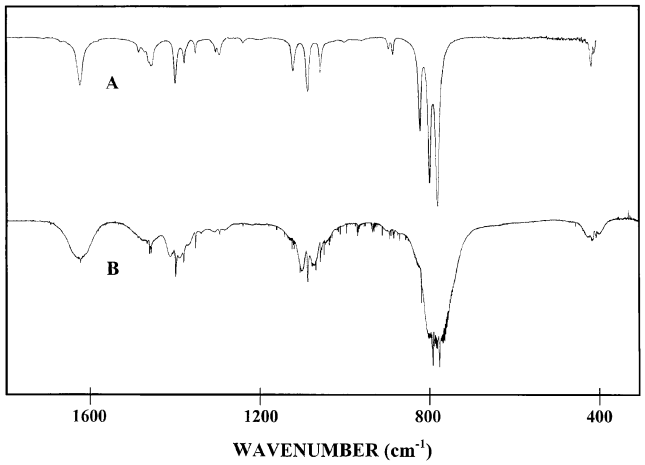

Figure 5. Comparison of infrared spectra of ethylamine: (A) krypton solution at −113 °C; (B) gas at ambient temperature.

values (Table 4), and the molecular sizes of the two rotamers are nearly the same, so the ΔH value obtained from the temperature-dependent Fourier transform infrared (FT-IR) study is expected to be reasonably close to the value for the gas.[24−28] However, dimerization from hydrogen bonding could present a problem.

Several conformer band pairs have been identified in the previous section. However, because of hydrogen bonding, bands associated with significant NH_2 motions for the gauche conformer were not utilized for the enthalpy determination, except for the NH_2 torsion. There is a clear shoulder on the low-frequency side of the gauche NH_2 torsion, which is due to a hydrogen-bonded species (Figure 2). Thus, the well-separated and well-defined bands used for the conformational stability study are those assigned to the CCN antisymmetric stretch (ν_{11}) at 1052 (trans) and 1082 (gauche) cm^{-1} and the CH_2 wag (ν_9) at 1347 and 1395 cm^{-1} (gauche), as well as the 881 and 795 cm^{-1} trans bands. From these bands, a total of eight sets of conformational band pairs along with the one in the far-infrared and their spectral intensity ratios were obtained in krypton solutions (Table 5). The intensities of the infrared bands were measured, and their ratios were determined at 5 °C intervals. By application of the van't Hoff equation $-\ln K = \Delta H/(RT) - \Delta S/R$, ΔH was determined from a plot of $-\ln K$ versus $1/T$, where $\Delta H/R$ is the slope of the line, and K is substituted with the intensity ratios between the trans and gauche bands. It was assumed that ΔH is not a function of temperature in the temperature range studied.

From these data, the enthalpy differences have been determined for each band pair, and the overall average with the statistical uncertainty is 54 ± 4 cm^{-1} (0.65 ± 0.05 kJ/mol) for the krypton solution, with the trans conformer being the more stable form (Table 5). Similarly, six band pairs were used for the enthalpy difference in the xenon solutions from which the overall average of 65 ± 3 (0.78 ± 0.04 kJ/mol) was obtained, again with the trans form being the more stable conformer. Since the bands in krypton solution are sharper with more easily determined baselines, it is believed that the ΔH from this rare gas is more accurate, although the slightly higher value in xenon could be due to the differences of the two solvents. The statistical error limit is given by the standard deviation of the measured areas of the intensity data. However, the error limit does not take into account the effect of the solute's small associations with the liquid noble gas solvent or the possible presence of overtones or combination bands in near-coincidence to the measured fundamentals.

TABLE 4: Structural Parameters[a] and Dipole Moments for the trans and gauche Conformers of Ethylamine

	trans			gauche		
parameter	MP2(full)/6-311+G(d,p)	electron diffraction[b]	adjusted r_0	MP2(full)/6-311+G(d,p)	electron diffraction[b]	adjusted r_0
$r(C_{1-C2})$	1.5280	1.531(6)	1.534	1.5209	1.524(6)	1.527
$r(C_{2-N3})$	1.4628	1.470(10)	1.466	1.4652	1.475(10)	1.470
$r(C_{1-H4})$	1.0948	1.107(6)	1.094	1.0933	1.107(6)	1.092
$r(C_{1-H5})$	1.0944	1.107(6)	1.093	1.0947	1.107(6)	1.094
$r(C_{1-H6})$	1.0944	1.107(6)	1.093	1.0922	1.107(6)	1.091
$r(C_{2-H7})$	1.0942	1.107(6)	1.098	1.1003	1.107(6)	1.106
$r(C_{2-H8})$	1.0942	1.107(6)	1.098	1.0940	1.107(6)	1.099
$r(N_{3-H9})$	1.0151	1.052	1.012	1.0146	1.052	0.998
$r(N_{3-H10})$	1.0151	1.052	1.012	1.0152	1.052	1.006
$\angle C_1C_2N_3$	115.50	115.0(3)	115.4	109.85	109.7(3)	110.1
$\angle H_4C_1C_2$	111.20	113.2(32)	111.8	111.00	113.2(32)	110.5
$\angle H_5C_1C_2$	110.62	113.2(32)	110.2	110.57	113.2(32)	110.1
$\angle H_6C_1C_2$	110.62	113.2(32)	110.2	110.14	113.2(32)	109.7
$\angle H_7C_2C_1$	109.64	113.2(32)	109.8	109.21	113.2(32)	110.2
$\angle H_8C_2C_1$	109.64	113.2(32)	109.8	109.58	113.2(32)	110.6
$\angle H_7C_2C_3$	107.57	113.2(32)	108.3	113.35	113.2(32)	113.2
$\angle H_8C_2C_3$	107.57	113.2(32)	108.3	107.61	113.2(32)	107.6
$\angle H_9N_3C_2$	110.18	111.1(50)	110.0	110.76	112.4(34)	111.5
$\angle H_{10}N_3C_2$	110.18	111.1(50)	110.0	109.81	112.4(34)	109.8
$\angle H_4C_1H_5$	108.14		108.5	107.87		108.3
$\angle H_4C_1H_6$	108.14		108.5	108.98		109.5
$\angle H_5C_1H_6$	107.99		108.4	108.20		108.6
$\angle H_9N_3H_{10}$	106.64		106.7	106.84		111.8
$\tau(H_4C_1C_2N_3)$	180		180	177.90		179.4
$\tau(H_5C_1C_2N_3)$	−59.81		−59.8	−62.42		−60.9
$\tau(H_6C_1C_2N_3)$	59.81		59.8	57.11		58.6
$\tau(H_7C_2C_1N_3)$	121.69		122.7	124.89		125.6
$\tau(H_8C_2C_1N_3)$	−121.69		−122.7	−118.02		−118.7
$\tau(H_9N_3C_2C_1)$	58.70		58.6	179.61		−172.6
$\tau(H_{10}N_3C_2C_1)$	−58.70		−58.6	61.84		62.9
$\lvert\mu_a\rvert$	1.255		1.057(6)[c]	0.098		0.11(1)[d]
$\lvert\mu_b\rvert$	0.846		0.764(9)[c]	0.764		0.65(1)[d]
$\lvert\mu_c\rvert$				1.228		1.014(15)[d]
$\lvert\mu_{tot}\rvert$	1.513		1.304(11)[c]	1.450		1.210(15)[d]

[a] Bond distances in Å, bond angles in degrees, and dipole moments in Debye. [b] Reference 8. [c] Dipole moments determined by microwave study, ref 10. [d] Dipole moments determined by microwave study, ref 6.

Structural Parameters

For a large number of substituted hydrocarbons, we have recently shown[29] that ab initio MP2(full)/6-311+G(d,p) calculations predict the C−H bond distances for more than 50 different C−H bonds to within ∼0.002 Å of the experimentally determined values obtained from "isolated" carbon−hydrogen stretching frequencies.[30] In addition, MP2(full)/6-311+G(d,p)-predicted C−C and C−N distances are generally within 0.006 Å of the adjusted r_0 structural parameters. Thus, by systematically adjusting MP2(full)/6-311+G(d,p)-predicted parameters to fit the previously reported microwave rotational constants[6,10,11] for various isotopomers, it is possible to obtain adjusted r_0 structural parameters by this method for both conformers of ethylamine. Because of the availability of rotational constants for a large number of isotopomers and the small size of the molecule, in principle, all of the structural parameters can be independently determined for the higher-symmetry trans conformer of ethylamine. However, such a fit reverses the order of the C−H distances of the methyl group, making the two equivalent out-of-plane C−H distances significantly longer than the in-plane one. This is against the well-acknowledged fact that the in-plane C−H distance is, in general, longer than the out-of-plane ones. Thus, two constraints have been set for the weighted least-squares fit of the rotational constants of the trans conformer, in that the ratio between the in-plane and out-of-plane C−H distances and the difference between the two angles of the methyl group are kept at the ab initio-predicted values.

The resulting adjusted r_0 structural parameters are listed in Table 4, along with the MP2(full)/6-311+G(d,p)-predicted values and the structures reported from a previous electron diffraction study.[8] The C−C and C−N distances are well within the error limits of the values reported from the electron diffraction study,[8] and they are predicted to be too short by 0.0056 and 0.0037 Å, respectively. In the electron diffraction study, to reduce independent variables in the fit of the radial distribution curve, all five C−H distances were set to be equal. However, the differences in the C−H distances can be determined in the present study. Most of the adjustments of hydrogen bending angles are less than 0.5° but with somewhat large changes for the $H_{7,8}C_2C_3$ and $H_7C_2H_8$ angles of the methylene group. A comparison of the resulting rotational constants from the adjusted r_0 parameters and the microwave rotational constants for the trans conformer are listed in Table 3S (Supporting Information). The average deviation of the fit is only 0.854 MHz for the A rotational constants and 0.400 MHz for the B and C constants.

The number of structural parameters for the gauche conformer nearly doubles because of the lack of a plane of symmetry. To reduce the number of independent variables, the structural parameters are separated into sets according to their types. Bond lengths in the same set keep their relative ratio, and bond angles and torsional angles in the same set keep their differences in degrees. This assumption is based on the generally accepted assumption that the errors from ab initio calculations are largely systematic. In addition, the constraints utilized on the methyl

TABLE 5: Temperature-Dependent Intensity Ratios between the trans and gauche Conformers of Ethylamine Dissolved in Liquid Krypton (top) and Xenon (bottom)

T (°C)	$1/T$ ($\times 10^{-3}$ K^{-1})	I_{1052t}/I_{1082g}	I_{1347t}/I_{1395g}	I_{1052t}/I_{1395g}	I_{1347t}/I_{1082g}	I_{795t}/I_{1082g}	I_{795t}/I_{1395g}	I_{881t}/I_{1082g}	I_{881t}/I_{1395g}	T (°C)	$1/T$ ($\times 10^{-3}$ K^{-1})	I_{265t}/I_{223g}
−105.0	5.9471	0.49956	0.24311	0.64340	0.18876	3.63423	4.68065	0.19957	0.25703	−113.4	6.2598	0.41595
−110.0	6.1293	0.49940	0.24213	0.63295	0.19104	3.68547	4.67101	0.21987	0.27866	−117.4	6.4205	0.40803
−115.0	6.3231	0.50028	0.24662	0.63494	0.19438	3.71977	4.71952	0.22871	0.29018	−121.4	6.5898	0.44561
−120.0	6.5295	0.50474	0.24953	0.64374	0.19565	3.75618	4.79061	0.23278	0.29689	−125.4	6.7682	0.45803
−125.0	6.7499	0.51269	0.25345	0.65397	0.19869	3.80895	4.85854	0.23727	0.30265	−129.4	6.9565	0.45916
−130.0	6.9857	0.52214	0.25617	0.67285	0.19879	3.85522	4.96804	0.24583	0.31679	−133.4	7.1556	0.47795
−135.0	7.2385	0.52768	0.25983	0.68079	0.20140	3.89801	5.02908	0.24849	0.32060	−137.4	7.3665	0.47236
−140.0	7.5103	0.54070	0.26349	0.70243	0.20282	3.98399	5.17571	0.24814	0.32237	−141.4	7.5901	0.47448
lin. coeff (R^2)		0.942	0.983	0.876	0.956	0.995	0.971	0.819	0.889			0.787
ΔH^a (cm^{-1})		37 ± 4	39 ± 2	44 ± 7	31 ± 3	39 ± 1	47 ± 3	86 ± 16	94 ± 13			80 ± 17

T (°C)	$1/T$ ($\times 10^{-3}$ K^{-1})	I_{1052t}/I_{1082g}	I_{1347t}/I_{1395g}	I_{1052t}/I_{1395g}	I_{1347t}/I_{1082g}	I_{795t}/I_{1082g}	I_{795t}/I_{1395g}
−55.0	4.5840	0.47706	0.21662	0.65387	0.15804	2.74731	3.76553
−60.0	4.6915	0.48471	0.22043	0.65838	0.16228	2.78399	3.78153
−65.0	4.8042	0.49375	0.22463	0.66440	0.16693	2.90873	3.91402
−70.0	4.9225	0.49614	0.22665	0.66841	0.16824	2.85101	3.84089
−75.0	5.0467	0.50079	0.23410	0.67824	0.17285	2.86625	3.88190
−80.0	5.1773	0.50676	0.23845	0.69220	0.17457	2.88889	3.94607
−85.0	5.3149	0.51038	0.24424	0.70479	0.17687	2.89599	3.99908
−90.0	5.4600	0.51113	0.24720	0.70650	0.17884	2.89719	4.00457
−95.0	5.6132	0.52093	0.24932	0.72365	0.17948	2.96185	4.11447
−100.0	5.7753	0.52577	0.25389	0.73759	0.18098	2.96240	4.15584
lin. coeff (R^2)		0.966	0.978	0.986	0.918	0.744	0.931
ΔH^a (cm^{-1})		52 ± 3	95 ± 5	72 ± 3	76 ± 8	36 ± 7	55 ± 5

[a] Overall enthalpy difference is 54 ± 4 cm^{-1} in the krypton solution and 65 ± 3 cm^{-1} in the xenon solution, with the trans conformer being more stable.

and methylene structures were the same as those used for the trans conformer. The resulting adjusted r_0 structural parameters for the gauche form are listed in Table 4, and the C−C and C−N distances are also within the error limits of the values reported from the electron diffraction study.[8] The "in-plane" N−H distance is predicted to be too long by 0.0163 Å, and the "out-of-plane" one is expected to be too long by 0.0088 Å. It should be noted that the CCN angle exhibits the largest difference in structure between the two conformers in which the value of the gauche form is 5.36° smaller than the that of the trans conformer. A comparison of the resulting rotational constants from the adjusted r_0 parameters and the microwave rotational constants for the gauche conformer are listed in Table 4S (Supporting Information). The average deviation of the fit is 2.313 MHz for the A rotational constants and 0.778 MHz for the B and C constants, where these values are about twice as large as those from the fit of the trans conformer, which is expected for the lower-symmetry gauche conformer.

Discussion

Since the enthalpy difference between the two conformers was predicted to be small, and relatively small experimentally determined values had been previously reported,[1,2,6−8] we utilized conformer pairs, which are much less susceptible to hydrogen bonding than the NH_2 modes. Additionally, we gathered data from two noble gas solutions to determine the experimental value. However, invariably, in the mid-infrared spectral region, there are possible interferences from overtone or combination bands, which can affect the variable-temperature infrared spectral intensity measurements, even in dilute noble gas solutions. Also, weak hydrogen bonding can cause dimer or oligomer associations, which can, in turn, affect infrared intensities. It is believed to be the reason the gauche band at 777 cm^{-1} could not be used for the ΔH determination. Thus, from the present study, the trans conformer has been identified as the more stable form.

It is possible to estimate the enthalpy difference between the two conformers by using the ab initio-predicted infrared intensities for the bands for each conformer and then measure the intensities at a single temperature. By using the 1052 cm^{-1} band, which has been assigned to the trans conformer, along with the gauche bands at 1082, 817, and 777 cm^{-1}, values of 120, 29, and 56 cm^{-1} are obtained for ΔH, again with the trans form being more stable. Similar results of 111, 21, and 63 cm^{-1} are obtained by using the trans band at 795 cm^{-1} with the same three gauche bands. The average value of these six estimates is 68 cm^{-1}, which supports the experimentally determined value of 54 ± 4 cm^{-1}. Finally, it should be noted that the ΔH was obtained from several of the bands that would be expected to participate in hydrogen bonding, and, in most cases, these gave values in the approximate range of ∼70 cm^{-1}. Also, five pairs of bands, which had poor correlation values ranging from 0.39 to 0.62, had values ranging from 11 to 51 cm^{-1} with an average value of 32 cm^{-1} for ΔH. Taking all these factors into consideration, the evidence that the trans conformer is the more stable form is overwhelming.

The enthalpy difference determined from the noble gas solutions is consistent with the ab initio calculations without diffuse functions, but Møller−Plesset perturbation methods with diffuse functions lead to the wrong order of conformational stability. The average ΔE predicted from the MP2 calculations is 57 cm^{-1}, which is only slightly lower than the average value of 65 cm^{-1} if the zero-point energy is included. However, with the larger basis sets, the agreement of the predicted ΔH and the experimental value is excellent. The value from the B3LYP calculations is significantly larger (120 cm^{-1}) without the diffuse functions but nearly zero with them (Table 3). Nevertheless, with energy differences so small, it appears difficult to predict whether diffuse functions should be used and at what levels of calculations will consistent results be obtained.[31]

We have redetermined the potential function governing the conformational interchange since the one reported earlier[2] had

TABLE 6: Far-Infrared NH_2 Torsional Transitions (cm^{-1}) of Gaseous Ethylamine

conformer	transition	observed[a]	calculated[b]	calcd − obsd
trans	1 ← 0	236.7	239.4	2.7
	2 ← 1	215.5	217.4	1.9
gauche	1± ← 0∓	218.0	217.3	−0.7
		218.0	217.3	−0.7
	2± ← 1∓	∼203	202.6	−0.4
		∼198	195.0	−3.0

[a] Reference 2. [b] Calculated using the potential coefficients listed in Table 7.

an enthalpy difference (230 cm^{-1}) between the two conformers much larger than the experimentally determined values or values predicted from ab initio calculations. Additionally, the internal rotational constants were calculated from structural parameters, which are significantly different from those obtained from the experimental data in the current study. Also, the observed isotopic shifts with deuteration of either the NH_2 or CH_3 groups (Figure 2) indicate minimal coupling between the two rotors, so a one-dimensional approximation of the conformational interchange seems more appropriate than the two-dimensional coupled approach previously used.[2] By using the Raman data of the gas,[1] the CH_3 and NH_2 torsional modes can be confidently assigned for the gauche conformers since the corresponding modes for the trans form will be antisymmetric modes that give rise to very broad nondescript lines in the Raman spectrum of the gas. Thus, the CH_3 torsional fundamental and first "hot band" (transition 2 ← 1) for the gauche conformer is confidently assigned at 258.8 and 248.5 cm^{-1}, respectively, with the NH_2 torsional fundamental appearing at 218 cm^{-1}. The first hot band for the gauche NH_2 torsion is split with a single broad Raman line at 200 cm^{-1}, which is the average of the two corresponding bands observed in the infrared spectra at 203 and 198 cm^{-1}. With the assignments for the CH_3 and NH_2 torsions for the gauche conformer, the corresponding modes for the trans form are readily assigned at 264.5 and 256.2 cm^{-1} for the CH_3 rotor, respectively, and 236.7 and 215.5 cm^{-1} for the first two NH_2 torsional modes.

With the assignment of the NH_2 torsional fundamental and one excited state for both the trans and gauche conformers, with splitting observed for the excited transition for the gauche form, along with the experimentally determined values for the enthalpy difference and the gauche dihedral angle, it should be possible to obtain values for six of the potential constants for a Fourier cosine series in the internal rotation angle θ: $V(\theta) = \sum_{i=1}^{6} V_i/2(1 - \cos i\theta)$, where θ and i are the torsional angle and foldness of the barrier, respectively. The internal rotation constant also varies as a function of the internal rotation angle, and it was approximated by another Fourier series: $F(\phi) = F_0 + \sum_{i=1}^{6} F_i \cos \phi$. The relaxation of the structural parameters, $B(\phi)$, during the internal rotation can be incorporated into the above equation by assuming that they are small periodic functions of the torsional angle of the general type: $B(\phi) = a + b \cos \phi + c \sin \phi$. The series approximating the internal rotation constants for ethylamine were determined by using structural parameters from the adjusted r_0 values. The potential coefficients V_1 through V_6 were calculated from the input of the frequencies for the two torsional transitions, the experimental ΔH value of 54 ± 5 cm^{-1}, the gauche dihedral angle of 120.72°, and the NH_2 internal rotation kinetic constant $F(\phi)$ (Table 7). However it was found that the V_6 term was very small (1 cm^{-1}) and the uncertainty (±13 cm^{-1}) was much larger than its value. Therefore, the V_6 term was dropped, and the final potential coefficients were obtained with reliably small uncertainties (Table 7). These

TABLE 7: Potential Coefficients and Barriers to Conformational Interchange (cm^{-1}) of Ethylamine

coefficients	experimental[a]	MP2(full)/6-311G(d,p)	coupled two-top model[b]
V_1	−207 ± 48	−78	316.5
V_2	320 ± 67	194	−11.3
V_3	1072 ± 25	922	713.7
V_4	55 ± 11	31	−25.0
V_5	−96 ± 28	−18	25.0
V_6		−16	−3.7
conformational enthalpy difference	54 ± 5	102	230
	potential barriers		
trans → gauche	1286	1068	774
gauche → trans	1232	973	546
gauche → gauche	715	731	827

[a] Calculated using $F_0 = 6.128099$, $F_1 = 0.011806$, $F_2 = 0.096290$, $F_3 = -0.002630$, $F_4 = 0.004667$, $F_5 = -0.000269$, and $F_6 = 0.000232$ cm^{-1}. [b] Reference 2.

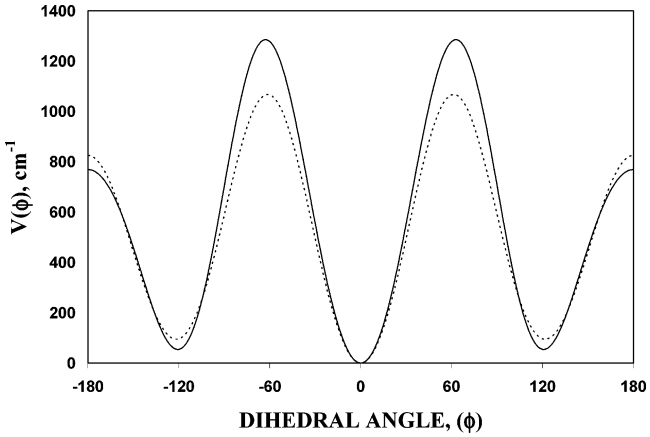

Figure 6. Potential function governing conformational interchange in ethylamine, with the solid curve being the experimentally determined potential function, and the dotted curve representing the MP2(full)/6-311G(d,p) calculations. The torsional dihedral angle of 0° corresponds to the trans conformer.

coefficients are compared to those from the MP2(full)/6-311G-(d,p)-calculated potential as well as previously reported values from the fit of the torsional transitions by a coupled two-top model.[2] The experimental and theoretical potential functions governing the conformational interchange of ethylamine are shown in Figure 6, where the experimentally determined barriers are the trans-to-gauche barrier at 1286 cm^{-1}, the gauche-to-trans barrier at 1232 cm^{-1}, and the gauche-to-gauche barrier at 715 cm^{-1} (Table 6). The MP2(full)/6-311G(d,p) calculations provide significantly smaller predictions of 1068 and 973 cm^{-1} for the trans-to-gauche and gauche-to-trans barriers, respectively, whereas the predicted gauche-to-gauche barrier of 731 cm^{-1} agrees with the experimental value. The function reported herein as well as that predicted from the ab initio calculations are significantly different from the one proposed from the two-top model, particularly for the trans-gauche barrier. The value we report of 1286 cm^{-1} is a little more than 200 cm^{-1} larger than the predicted barrier, which is consistent with the differences frequently found for methyl rotor barriers at this level and basis set for these calculations. However, the previously reported[2] value of 774 cm^{-1} seems entirely too small for this barrier, but the earlier investigators[2] pointed out that the relative heights of the trans and gauche minima were not particularly sensitive to the observed frequencies in the well. In fact, they[2] suggest that this energy difference may depend on the model for the internal

rotor, that is, its geometry, internal rotation coordinate, and the reduced mass, for example. Therefore, the 230 cm^{-1} energy difference between the two minima leads to a predicted splitting of 1.3 cm^{-1} for the second energy level, with the third one above the barrier, which is not consistent with the observed frequencies.

With small differences in the structural parameters between the two conformers, one would not expect significant differences in the force constants. Most of the force constant differences between the two conformers are less than 5%, but there are some notable exceptions. The largest difference is the C_1C_2 stretching force constant, where the value is 6.2% larger for the gauche conformer (4.392 mdyn/Å) than it is for the trans conformer (4.135 mdyn/Å) (Table 1S, Supporting Information). Similarly, the force constant associated with $C_1C_2N_3$ bend for the gauche (0.857 mdyn·Å·rad^{-2}) conformer is 5.9% larger than the one for the trans conformer (0.809 mdyn·Å·rad^{-2}). These differences are expected since the skeletal modes are more sensitive to conformational interchange, with the significantly higher fundamental frequencies of the gauche conformer agreeing well with the significantly larger force constants.

Since the mixing of CH_3 and NH_2 torsional modes for the gauche conformer are not nearly as extensive as those for the trans form, it should be possible to obtain the barrier to methyl rotation for this conformer. The mixing is further reduced for the $CH_3CH_2ND_2$ isotopomer, and the methyl torsional frequencies from the Raman data[1] have been used since there is the fundamental and three "hot bands". From these torsional data, the periodic 3-fold barrier, V_3, to internal rotation of the CH_3 group can be determined by utilizing the general equation $V_3 = 9/4 \cdot F \cdot s$, where F (in cm^{-1}) is given by $h/8\pi^2 cI_r$, and I_r is the reduced moment of inertia of the CH_3 top. The dimensionless parameter of the Mathieu equation, s, is indirectly determined from the observed frequencies. The F number was determined from the r_0 structural parameters to have a value of 6.395 cm^{-1}. Initially, we utilized both V_3 and V_6 terms, but the V_6 term was less than 2 cm^{-1} with an uncertainty of 1.6 cm^{-1}, so it was dropped. The final determined V_3 barrier is 1241 $\pm$ 4 cm^{-1}, which should be quite accurate since the frequencies of five transitions were used, with the latter two near the top of the well. This value is in excellent agreement with the predicted value (1244 cm^{-1}) from the MP4(SDTQ)/6-311G(2d,2p) calculations or the one 8 wavenumbers higher with the similar calculation with diffuse functions (Table 5S, Supporting Information). Also, it is only about 20 cm^{-1} lower than most of the predicted values from the MP2(full) calculations. The CH_3 barrier for the trans conformer is expected to be about 40 cm^{-1} higher (1281 cm^{-1}) on the basis of the difference between the torsional fundamental, but clearly there is more mixing of CH_3 and NH_2 torsional modes based on the PEDs.

By utilization of scaling factors of 0.92 for CH and NH stretches, 1.0 for CC and CN stretches and the CCN bend, and 0.96 for all other coordinates, the predicted frequencies for the fundamentals of the trans conformer have an average deviation of 7.3 cm^{-1}, which represents a relative error of only 0.44%. For the gauche conformer, the predicted frequencies for the fundamentals have an average deviation of 8.9 cm^{-1} and a relative error of 0.54%. The fundamentals with the largest discrepancies between the predicted and the observed values are ν_{13} (NH_2 wag) and ν_{21} (NH_2 twist). We have found for a series of amines and hydrazines[32−36] that ab initio (at this level and basis set)-calculated NH_2 wag frequencies are systematically overestimated by a large margin. Thus, the force constants involving the ∠CNH internal coordinate have to be scaled by a factor significantly smaller than the ones for other hydrogen bends to properly adjust the predicted frequencies. However, such small scaling factors inevitably lead to significant underestimates of NH_2 deformation and NH_2 twist frequencies. However, the choice of scaling factor does not complicate the assignment of the NH_2 wag (ν_{13}) for ethylamine since this mode is predicted to be the most intense band of the entire infrared spectrum, with intensity an order of magnitude larger than other bands in the fingerprint spectral region.

The PEDs are relatively pure for the trans conformer for a molecule with only C_s symmetry. The major exceptions for the A′ modes are for ν_{10}, CH_3 rock, (35% S_{10}, 22% S_{12}, 15% S_{14}, and 11% S_{11}), ν_{12}, CCN symmetric stretch (40% S_{12}, 36% S_{10}, and 15% S_{13}), and ν_{13}, NH_2 wag (49% S_{13}, 33% S_{12}, and 17% S_5), where the first one has significant contributions from four symmetry coordinates. In the A″ species, there is major mixing of ν_{20}, CH_3 rock (27% S_{20}, 23% S_{21}, 22% S_{22}, and 22% S_{19}) and ν_{21}, NH_2 twist (38% S_{21}, 31% S_{20}, 16% S_{19}, and 12% S_{22}). The remaining stretching and bending modes have contributions of 50% or more of the symmetry coordinates used as the description of the fundamental vibration. For the gauche conformer, the mixing is slightly more extensive.

The shoulder at 212 cm^{-1} on the NH_2 torsional fundamental at 223 cm^{-1} in the krypton is undoubtedly due to a hydrogen-bonded dimer of the gauche conformer. Therefore, the enthalpy difference between the 223 and 212 cm^{-1} bands was determined from the relative intensity of these two bands, and a value of 466 $\pm$ 45 cm^{-1} was obtained. This value is consistent with the value of 530 $\pm$ 29 cm^{-1} (6.34 $\pm$ 0.35 kJ/mol) that was obtained for the hydrogen-bond enthalpy in methylamine.[31] It is believed that this relatively strong hydrogen bond for the gauche conformer is the reason that the fundamentals involving the NH_2 wagging motions could not be used to obtain enthalpy differences between the two conformers. An ab initio study of the dimer formation of the trans and gauche conformers could possibly provide an explanation of why the hydrogen bonding of the gauche conformer appears to be much stronger than that in the trans form. Also, ab initio-predicted energy differences with much larger basis sets and higher levels could provide information on the desirability of using or not using diffuse functions for predicting conformational stabilities for these types of molecules. More extensive theoretical calculations of these types of molecules would be of interest since, with diffuse functions, the gauche conformer was clearly favored.

Acknowledgment. J.R.D. acknowledges the University of Missouri-Kansas City for a Faculty Fellowship award for partial financial support of this research. W.A.H. and B.J.V. thank the Flemish Community for financial support through the Special Research Fund (BOF) and the Scientific Affairs Division of NATO for travel funds between our two laboratories.

Supporting Information Available: Tables listing the scaled diagonal force constants calculated from B3LYP/6-311++G(3df,3pd) for ethylamine (1S); the symmetry coordinates for ethylamine (2S); the rotational constants obtained from ab initio MP2(full)/6-311+G(d,p) predictions and microwave spectra, and the adjusted structural parameters for trans (3S) and gauche (4S) ethylamine; and the calculated barriers to methyl rotation for the trans and gauche conformers. Figure (1S) showing the predicted A-, B-, and C-type gas-phase infrared band contours for both trans and gauche ethylamine. This material is available free of charge via the Internet at http://pubs.acs.org.

References and Notes

(1) Durig, J. R.; Li, Y. S. *J. Chem. Phys.* **1975**, *63*, 4110.
(2) Tsuboi, M.; Tamagake, K.; Hirakawa, A. Y.; Yamaguchi, J.; Nakagawa, H.; Manocha, A. S.; Tuazon, E. C.; Fateley, W. G. *J. Chem. Phys.* **1975**, *63*, 5177.
(3) Manocha, A. S.; Tuazon, E. C.; Fateley, W. G. *J. Phys. Chem.* **1974**, *78*, 803.
(4) Radom, L.; Hehre, W. J.; Pople, J. A. *J. Am. Chem. Soc.* **1972**, *94*, 2371.
(5) Tsuboi, M.; Hirakawa, A. Y.; Tamagake, K. *Nippon Kagaku Zasshi* **1968**, *89*, 821.
(6) Fischer, E.; Botskor, I. *J. Mol. Spectrosc.* **1984**, *104*, 226.
(7) Hamada, Y.; Hashiguchi, K.; Hirakawa, A. Y.; Tsuboi, M.; Nakata, M.; Tasumi, M.; Kato, S.; Morokuma, K. *J. Mol. Spectrosc.* **1983**, *102*, 123.
(8) Hamada, Y.; Tsuboi, M.; Yamanouchi, K.; Kuchitsu, K. *J. Mol. Struct.* **1986**, *146*, 253.
(9) Zeroka, D.; Jensen J. O.; Samuels, A. C. *J. Phys. Chem. A* **1998**, *102*, 6571.
(10) Fischer, E.; Botskor, I. *J. Mol. Spectrosc.* **1982**, *91*, 116.
(11) Fischer, E. Thesis, University of Ulm, 1984.
(12) Kruger, P. J.; Jan, J. *Can. J. Chem.* **1970**, *48*, 3229.
(13) Konarski, J. *J. Mol. Struct.* **1971**, *7*, 337.
(14) Konarski, J. *Chem. Phys. Lett.* **1971**, *12*, 249.
(15) Wolff, H.; Wolff, E.; Schmidt, U. *Spectrochim. Acta* **1991**, *47A*, 165.
(16) Durig, J. R.; Zheng, C.; Guirgis, G. A.; Wurrey, C. J. *J. Phys. Chem. A* **2005**, *109*, 1650.
(17) Miller, F. A.; Harney, B. M. *Appl. Spectrosc.* **1970**, *24*, 291.
(18) Frisch, M. J.; Trucks, G. W.; Schlegel, H. B.; Scuseria, G. E.; Robb, M. A.; Cheeseman, J. R.; Montgomery, J. A., Jr; Vreven, T.; Kudin, K. N.; Burant, J. C.; Millam, J. M.; Iyengar, S. S.; Tomasi, J.; Barone, V.; Mennucci, B.; Cossi, M.; Scalmani, G.; Rega, N.; Petersson, G. A.; Nakatsuji, H.; Hada, M.; Ehara, M.; Toyota, K.; Fukuda, R.; Hasegawa, J.; Ishida, M.; Nakajima, T.; Honda, Y.; Kitao, O.; Nakai, H.; Klene, M.; Li, X.; Knox, J. E.; Hratchian, H. P.; Cross, J. B.; Adamo, C.; Jaramillo, J.; Gomperts, R.; Stratmann, R. E.; Yazyev, O.; Austin, A. J.; Cammi, R.; Pomelli, C.; Ochterski, J. W.; Ayala, P. Y.; Morokuma, K.; Voth, G. A.; Salvador, P.; Dannenberg, J. J.; Zakrzewski, V. G.; Dapprich, S.; Daniels, A. D.; Strain, M. C.; Farkas, O.; Malick, D. K.; Rabuck, A. D.; Raghavachari, K.; Foresman, J. B.; Ortiz, J. V.; Cui, Q.; Baboul, A. G.; Clifford, S.; Cioslowski, J.; Stefanov, B. B.; Liu, G.; Liashenko, A.; Piskorz, P.; Komaromi, I.; Martin, R. L.; Fox, D. J.; Keith, T.; Al-Laham, M. A.; Peng, C. Y.; Nanayakkara, A.; Challacombe, M.; Gill, P. M. W.; Johnson, B.; Chen, W.; Wong, M. W.; Gonzalez, C.; Pople, J. A. *Gaussian 03*, revision B.04; Gaussian, Inc.: Pittsburgh, PA, 2003.
(19) Pulay, P. *Mol. Phys.* **1969**, *17*, 197.
(20) Guirgis, G. A.; Zhu, X.; Yu, Z.; Durig, J. R. *J. Phys. Chem. A* **2000**, *104*, 4383.
(21) Frisch, M. J.; Yamaguchi, Y.; Gaw, J. F.; Schaefer, H. F., III; Binkley, J. S. *J. Chem. Phys.* **1986**, *84*, 531.
(22) Amos, R. D. *Chem. Phys. Lett.* **1986**, *124*, 376.
(23) Zeroka, D.; Jensen, J. O.; Samuels, A. C. *J. Mol. Struct.* **1999**, *465*, 119.
(24) Herrebout, W. A.; van der Veken, B. J. *J. Phys. Chem.* **1996**, *100*, 9671.
(25) Herrebout, W. A.; van der Veken, B. J.; Wang, A.; Durig, J. R. *J. Phys. Chem.* **1995**, *99*, 578.
(26) Bulanin, M. O. *J. Mol. Struct.* **1995**, *347*, 73.
(27) van der Veken, B. J.; DeMunck, F. R. *J. Chem. Phys.* **1992**, *97*, 3060.
(28) Bulanin, M. O. *J. Mol. Struct.* **1973**, *19*, 59.
(29) Durig, J. R.; Ng, K. W.; Zheng, C.; Shen, S. *Struct. Chem.* **2004**, *15*, 149.
(30) McKean, D. C. *J. Mol. Struct.* **1984**, *113*, 251.
(31) Galabov, B.; Kenny, J. P.; Schaefer, H. F., III; Durig, J. R. *J. Phys. Chem. A* **2002**, *106*, 3625.
(32) Durig, J. R.; Zheng, C. *Struct. Chem.* **2001**, *12*, 137.
(33) Durig, J. R.; Gounev, T. K.; Zheng, C.; Choulakian, A.; Verma, V. N. *J. Phys. Chem. A* **2002**, *106*, 3395.
(34) Durig, J. R.; Zheng, C. *J. Mol. Struct.* **2004**, *690*, 31.
(35) Durig, J. R.; Zheng, C.; Herrebout, W. A.; van der Veken, B. J. *J. Mol. Struct.* **2002**, *641*, 207.
(36) Herrebout, W. A.; Zheng, C.; van der Veken, B. J.; Durig, J. R. *J. Mol. Struct.* **2003**, *645*, 109.